eNeuro

Research Article: New Research | Neuronal Excitability

Secondary Ammonium Agonists Make Dual Cation-# Interactions in #4#2 Nicotinic Receptors

Ammoniums Form Dual Cation-#'s in #4#2 nAChRs

Michael R Post[1], Gabrielle S Tender[1], Henry A Lester[2] and Dennis A Dougherty[1]

[1]*Division of Chemistry and Chemical Engineering, California Institute of Technology, Pasadena, CA USA*
[2]*Division of Biology and Biological Engineering, California Institute of Technology, Pasadena, CA USA*

DOI: 10.1523/ENEURO.0032-17.2017

Received: 26 January 2017

Revised: 28 February 2017

Accepted: 2 March 2017

Published: 17 March 2017

Author Contributions: MRP, GST, HAL, and DAD designed research; MRP and GST performed research and analyzed data; MRP wrote the paper.

Funding: HHS | NIH | National Institute of Neurological Disorders and Stroke (NINDS)
100000065
NS34407

Funding: HHS | NIH | National Institute on Drug Abuse (NIDA)
100000026
DA 019375

Conflict of Interest: Authors report no conflict of interest.

HHS | NIH | National Institute of Neurological Disorders and Stroke (NINDS) (100000065, grant no. NS34407); HHS | NIH | National Institute on Drug Abuse (NIDA)(funding id. 100000026, grand no. DA 019375) Beckman Institute.

Correspondence should be addressed to Dennis A Dougherty, MC 164-30, 1200 E California Blvd, Pasadena, CA 91125, USA. E-mail: dadougherty@caltech.edu

Cite as: eNeuro 2017; 10.1523/ENEURO.0032-17.2017

1. **Title:**

Secondary Ammonium Agonists Make Dual Cation-π Interactions in α4β2 Nicotinic Receptors

2. **Abbreviated Title:**

2° Ammoniums Form Dual Cation-π's in α4β2 nAChRs

3. **Authors and Affiliations:**

Michael R Post[1], Gabrielle S Tender[1], Henry A Lester[2], Dennis A Dougherty[1]
[1]Division of Chemistry and Chemical Engineering, California Institute of Technology, Pasadena, CA, USA
[2]Division of Biology and Biological Engineering, California Institute of Technology, Pasadena, CA, USA

4. **Author Contributions**

MRP, GST, HAL, and DAD designed research; MRP and GST performed research and analyzed data; MRP wrote the paper

5. **Correspondence should be addressed to**

Dennis A Dougherty
MC 164-30
1200 E California Blvd
Pasadena, CA 91125
dadoc@caltech.edu

6. **Number of Figures:** 5
7. **Number of Tables:** 4
8. **Number of Multimedia**: 0
9. **Number of Words Abstract:** 139
10. **Number of words for Significance Statement:** 94
11. **Number of Words for Introduction:** 432
12. **Number of Words for Results & Discussion:** 881+593 = 1474
13. **Acknowledgements**

We thank the NIH (NS 34407, DA 019375) and the Beckman Institute at Caltech for support of this work. MRP was supported by an NIH/NRSA training grant: 5 T32 GM07616.

14. **Conflict of Interest:** None
15. **Funding Sources:** NIH; Beckman Institute

Secondary Ammonium Agonists Make Dual Cation-π Interactions in α4β2 Nicotinic Receptors

Abstract

A cation-π interaction between the ammonium group of an agonist and a conserved tryptophan termed TrpB is a near universal feature of agonist binding to nicotinic acetylcholine receptors (nAChRs). TrpB is one of five residues that form the aromatic box of the agonist binding site, and for the prototype agonists ACh and nicotine, only TrpB makes a functional cation-π interaction. We report that, in addition to TrpB, a significant cation-π interaction is made to a second aromatic – TyrC2 – by the agonists metanicotine, TC299423, varenicline, and nornicotine. A common structural feature of these agonists – and a distinction from ACh and nicotine – is a protonated secondary amine that provides the cation for the cation-π interaction. These results indicate a distinction in binding modes between agonists with subtly different structures that may provide guidance for the development of subtype-selective agonists of nAChRs.

Significance Statement

The α4β2 nicotinic acetylcholine receptor binding site is made of several loops contributing five aromatic residues. Here we show four secondary ammonium agonists – TC299423, metanicotine, varenicline, and nornicotine – make a cation-π interaction with TyrC2 in addition to the canonical cation-π interaction with TrpB. The prototypical agonists acetylcholine (a quaternary ammonium), and nicotine (a tertiary ammonium) only make a cation-π interaction with TrpB. This result indicates a new binding mode for agonists with only subtle

structural differences, and suggests that a more compact cation allows for greater interaction with Loop C in the binding site.

Introduction

The neuronal nicotinic acetylcholine receptors (nAChR) are members of the Cys-loop ligand-gated ion channel family and are established therapeutic targets for nicotine addiction, as well as possible targets for Parkinson's disease, Alzheimer's disease, pain, and other neural disorders (Romanelli et al., 2007). The receptors are pentamers, and eleven known subunits – α2-7,9,10 and β2-4 – combine to form distinct subtypes (Gotti et al., 2006; Le Novère et al., 2002; Millar, 2003; Zoli et al., 2015). The nAChR binding site lies at the extracellular α-β interface, and it contains an aromatic box motif that binds the cationic moiety of the agonist through a cation-π interaction (**Fig. 1)** (Dougherty, 1996, 2013; Van Arnam and Dougherty, 2014). Five aromatic residues are contributed by four loops – TyrA, Trp B, TyrC1, TyrC2, and TrpD (Corringer et al., 2000). In many studies of ligands binding to nAChRs, TrpB forms a functionally important cation-π interaction, while the other aromatics apparently play other roles (Blum et al., 2010, 2013; Puskar et al., 2012; Tavares et al., 2012; Van Arnam and Dougherty, 2014; Xiu et al., 2009).

A major goal in nAChR research is to develop agonists that target specific subtypes (Dineley et al., 2015; Holladay et al., 1997; Quik and Wonnacott, 2011). For example, the α4β2-containing subtypes are expressed throughout the brain and are most associated with several aspects of nicotine addiction (De Biasi and Dani, 2011). The α6β2-containing subtypes have a more restricted distribution. They occur on dopaminergic neurons, where they have been associated with reward-related behavior and Parkinson's disease, as well as on medial habenula neurons, which play a role in aversive behavior (Henderson et al., 2014; Jackson et al., 2013;

Quik and McIntosh, 2006; Zuo et al., 2016). Finding agonists that meaningfully distinguish between the α4β2 and α6β2 interfaces is an unsolved challenge, but metanicotine (rivanicline, TC-2403, or RJR-2403) and TC299423, have been found to preferentially activate α4β2- and α6β2-containing subtypes, respectively (Drenan et al., 2008; Grady et al., 2010; Wall, 2015; Xiao et al., 2011).

Previous analysis of TC299423 at α6β2 showed an unusual binding pattern, in that the agonist does not make a functional cation-π interaction with TrpB or any other aromatic box residue (Post et al., 2015); thus, a unique binding mode may contribute to its subtype selectivity. Here, TC299423 and other agonists were studied at the more extensively characterized α4β2 receptor, in order to see if the unusual binding pattern persists. Several agonists were found to make cation-π interactions with both TrpB and TyrC2, and we show that this dual cation-π feature is a more general trend amongst secondary ammonium agonists (**Fig. 2**) at α4β2.

Materials and Methods

Molecular Biology

Rat α4 and β2 subunits were used as the basis for the constructs. The L9'A mutation in the α4 M2 transmembrane domain, at the gate of the channel, was incorporated in order to amplify signal by shifting the stability of the channel partiially toward the active state. This α4L'Aβ2 construct is described as wild-type and/or α4β2 throughout the report for clarity in comparing non-canonical mutations made to the binding site, which is over 60 Å away from the channel gate. All constructs were in the pGEMhe vector, a cDNA plasmid optimized for protein expression in *Xenopus* oocytes. Site-directed mutagenesis was performed by PCR using the Stratagene QuikChange protocol, and primers ordered from Integrated DNA Technologies (Coralville, IA). Circular cDNA was linearized with SbfI (New England Biolabs, Ipswich, MA) and then transcribed *in vitro* using T7 mMessage mMachine kit (Life Technologies, Santa Clara, CA), with a purification step after each process (Qiagen, Valencia, CA). Final concentrations were quantified by UV spectroscopy.

Ion Channel Expression

Xenopus laevis oocytes (stage V to VI) were sourced from both an institute facility and Ecocyte Bio Science (Austin, TX). Oocytes were injected with 50 nL solution containing either 5 or 10 ng mRNA, injected in a 1:2 α4:β2 ratio **in order to control for a pure population of the $(\alpha4L9'A)_2(\beta2)_3$ stoichiometry. The alternative stoichiometry $(\alpha4)_3(\beta2)_2$ has a much lower EC_{50} due to the extra L9'A mutation. We therefore avoided a mixed population containing both stoichiometries**. Cells were incubated 24-48 hours at 18°C in ND96 solution (96 mM NaCl, 2mM KCl, 1 mM $MgCl_2$, and 5mM HEPES, pH 7.5) enriched with theophylline, sodium pyruvate, and gentamycin.

Non-canonical Amino Acid Incorporation

The cyanomethylester form of NVOC-protected tryptophan and phenylalanine analogues was coupled to dinucleotide dCA and enzymatically ligated to UAG-suppressor 74-mer THG73 $tRNA_{CUA}$. The product was verified by MALDI time-of-flight mass spectrometry on a 3-hydroxypicolinic acid matrix. The non-canonical amino acid-coupled tRNA was deprotected by photolysis either on a 500 W Hg/Xe arc lam, filtered with Schott WG-320 and UG-11 filters, or with an M365LP1 365 nm 1150 mW LED lamp (Thor Labs, Newton, NJ) immediately prior to coinjection with mRNA containing the UAG mutation at the site of interest. mRNA and tRNA were typically injected in a 1:1 or 1:2 volume ratio in a total volume of 50 or 75 nL respectively, so that 25 ng of mRNA was injected per cell. In cases where observed agonist-induced currents were low after 48-hour incubation – likely due to low protein expression – a second injection of mRNA and tRNA was performed after 24 hours. The fidelity of non-canonical amino acid incorporation was confirmed at Trp with a wild-type recovery experiment where tryptophan was loaded onto tRNA. If this experiment yielded similar to EC_{50} to wild-type, then the cell incorporated the charged residue and nothing else. This was accomplished with the Tyr sites by comparing tRNA charged with Phe to a conventional Tyr-Phe mutation. A read-through/reaminoacylation test served as a negative control by injecting unacylated full-length 76-mer tRNA. Lack of current proved no detectable reaminoacylation at the suppression site.

Whole-Cell Electrophysiological Characterization

(S)-nornicotine hydrochloride was purchased from Matrix Scientific (Columbia, SC), while varenicline (Pfizer), metanicotine and TC299423 (Targacept) were generous gifts. Agonist-induced currents were recorded in TEVC mode using the OpusXpress 6000A (Molecular Devices, Sunnyvale, CA) at a holding potential of -60 mV in a running buffer of Ca^{2+}-free ND96**, which since α4β2 is Ca^{2+} permeable, prevents interference from Ca^{2+}-activated channels endogenous to the oocyte**. Agonists were

prepared in Ca^{2+}-free ND96 and delivered to cells via a 1 mL application over 15 sec followed by a 2 min wash. Data from dose-response experiments**, representative traces are shown in Figure 5,** were normalized, averaged, and fit to the Hill equation using Kaleidagraph (Synergy Software, Reading PA). In data tables, N is the total number of oocytes analyzed, and cells from different frogs on at least two different days were used for each point. Fluorination plots are visualized here with Prism (GraphPad Software, La Jolla, CA). EC_{50} and Hill coefficient errors are presented as SEM.

Results

Binding Studies of TC299423 and metanicotine at α4β2

All studies here used the previously described $(\alpha L9'A)_2(\beta 2)_3$ receptor (Kuryatov, 2005; Nelson et al., 2003). TC299423 was first probed for cation-π interactions at TrpB and TyrC2 (TyrA, TyrC1, and TrpD have never been implicated in a cation-π interaction). In these experiments, the site of the aromatic residue of interest is mutated to a TAG stop codon. mRNA made *in vitro* is injected into *Xenopus* oocytes alongside a bioorthogonal $tRNA_{CUA}$ that has been chemically appended to the non-canonical amino acid of interest. To probe for an agonist cation-π interaction, a series of residues with electron-withdrawing groups that weaken the interaction is used. Typically, fluorotryptophans (F_nTrp) are used to probe Trp and fluorophenylalanines (F_nPhe) are used to probe Tyr (fluorinating tyrosine causes the phenol group to deprotonate at physiological pH). The endpoints of the two series – F_4-Trp and F_3-Phe – are both thought to approximate a situation in which the dominant electrostatic component of the cation-π interaction has been completely removed, allowing a semi-quantitative comparison of Trp and Tyr residues. Any change in binding is revealed by a changed EC_{50} value, monitored by two-electrode voltage clamp electrophysiology dose-response experiments. If the interaction is weakened by these substitutions, EC_{50} correspondingly increases. This change is visualized in so-called fluorination

plots of the log of the fold-shift in EC_{50} against the calculated gas-phase cation-π interaction strength.

At TrpB, TC299423 showed an increase in EC_{50} with each additional fluorine substituent on the ring (**Table 1**), but the maximum fold-shift in EC_{50} observed at F_4Trp was only 6.6-fold. While this is a modest loss of function – ACh experiences a 66-fold loss of function at F_4Trp in α4β2 (Xiu et al., 2009) – there is nevertheless a linear trend in the fluorination plot (**Fig 3**). Thus, it can be said that TC299423 makes a functional, if modest, cation-π interaction with TrpB in α4β2.

Table 1. TC299423

TrpB	EC_{50} (μM)	n_H	I_{max} (μA)	Fold Shift	N
Trp	0.023 ± 0.0009	1.4 ± 0.06	0.22 - 1.46	1	15
F_1Trp	0.043 ± 0.0008	1.3 ± 0.03	0.12 - 1.2	1.8	11
F_2Trp	0.052 ± 0.001	1.2 ± 0.04	0.05 - 0.62	2.2	14
F_3Trp	0.13 ± 0.003	1.2 ± 0.03	0.11 - 1.41	5.5	12
F_4Trp	0.15 ± 0.007	1.1 ± 0.05	0.15 - 0.77	6.6	14
TyrC2	**EC_{50} (μM)**	**n_H**	**I_{max} (μA)**	**Fold Shift**	**N**
Phe	0.098 ± 0.003	1.1 ± 0.03	0.06 - 1.08	1	17
F_1Phe	0.14 ± 0.005	1.2 ± 0.04	0.05 - 0.38	1.5	12
F_2Phe	1.6 ± 0.07	1.3 ± 0.06	0.05 - 0.57	16	9
F_3Phe	3.0 ± 0.25	1.3 ± 0.11	0.07 - 0.18	30	7

TyrC2 was then probed for a cation-π interaction with TC299423 and showed an unexpected trend, with F_3Phe substitution resulting in a 30-fold increase in EC_{50}. When presented as a fluorination plot (**Fig 4**), these results show a linear trend, showing that in addition to a cation-π interaction with TrpB, TC299423 makes a functional – and energetically more significant - cation-π interaction at TyrC2.

Metanicotine, an isomer of nicotine in which the pyrrolidine ring has been opened, has antinociceptive effects in mice and is more potent and efficacious than ACh at α4β2 receptors

(Damaj et al., 1999; Papke et al., 2000). When analyzed via a fluorination series at TrpB in α4β2, metanicotine displayed a functional cation-π interaction, with a linear fluorination plot and F_4Trp resulting in a 25-fold shift in EC_{50} (**Table 2**, **Fig 3**). TyrC2 also shows a linear fluorination plot, with the F_3Phe mutation causing a 51-fold shift relative to Phe (**Fig 4**). TyrA was probed and showed no meaningful changes in metanicotine EC_{50} upon fluorination (**Table 2**, nicotine and ACh also showed no meaningful shifts in EC_{50} at this site (Xiu et al., 2009). Thus, metanicotine also forms dual, functional cation-π interactions at TrpB and TyrC2 in α4β2.

Table 2. Metanicotine

TrpB	EC_{50} (μM)	n_H	I_{max} (μA)	Fold Shift	N
Trp	0.64 ± 0.02	1.3 ± 0.0	0.08 - 0.89	1	13
F_1Trp	0.79 ± 0.02	1.4 ± 0.0	0.12 - 0.80	1.2	16
F_2Trp	3.6 ± 0.1	1.5 ± 0.1	0.15 - 0.56	5.6	14
F_3Trp	13 ± 1	1.6 ± 0.1	0.07 - 0.30	20	12
F_4Trp	16 ± 2	1.3 ± 0.1	0.03 - 0.11	25	12

TyrA	EC_{50} (μM)	n_H	I_{max} (μA)	Fold Shift	N
Phe	19 ± 5	1.1 ± 0.2	0.02 - 0.16	1	7
F_3Phe	17 ± 2	1.3 ± 0.1	0.01 - 0.03	0.9	6

TyrC2	EC_{50} (μM)	n_H	I_{max} (μA)	Fold Shift	N
Phe	0.41 ± 0.03	1.2 ± 0.07	0.06 - 2.78	1	17
F_1Phe	0.86 ± 0.06	1.2 ± 0.08	0.04 - 0.07	2.1	11
F_2Phe	11 ± 1	0.6 ± 0.1	0.03 - 0.13	27	8
F_3Phe	21 ± 1	1.4 ± 0.2	0.04 - 0.24	51	12

Both metanicotine and TC299423 are typical nicotinic pharmacophores in that they have a cationic amine moiety, a hydrogen bond donor associated with that amine, and a hydrogen bond acceptor several angstroms away (Blum et al., 2010). In contrast to the tertiary ammonium nicotine and the quaternary ammonium ACh, metanicotine and TC299423are both secondary

187 ammonium ions. Thus, to test whether this feature was associated with the novel dual cation-π
188 interaction, additional secondary amine agonists were analyzed.

189 *Establishing a Binding Trend for Secondary Amines*

190 Varenicline (Chantix®) is a smoking cessation drug that is thought to work by serving as
191 a partial agonist to α4β2 (Coe et al., 2005a, 2005b) It has a secondary ammonium as its cationic
192 center. This drug has previously been shown to form a cation-π interaction at TrpB in α4β2
193 (Tavares et al., 2012), with a 23-fold shift in EC_{50} at F_4Trp (**Table 3, Fig 3**), but had not been
194 analyzed at TyrC2.

Table 3. Varenicline

TrpB*	EC_{50} (μM)	n_H	Fold Shift	N
Trp	0.0024 ± 0.0001	1.2 ± 0.1	1	15
F_1Trp	0.0057 ± 0.0002	1.2 ± 0.1	2.4	11
F_2Trp	0.0057 ± 0.0021	1.2 ± 0.1	2.4	14
F_3Trp	0.027 ± 0.001	1.3 ± 0.1	11	12
F_4Trp	0.056 ± 0.005	1.1 ± 0.1	23	14

TyrC2	EC_{50} (μM)	n_H	I_{max} (μA)	Fold Shift	N
Phe	0.0014 ± 0.0002	1.3 ± 0.14	0.04 - 0.14	1	10
F_1Phe	0.0020 ± 0.00009	1.5 ± 0.09	0.02 - 0.08	1.4	8
F_2Phe	0.011 ± 0.00097	1.2 ± 0.11	0.02 - 0.1	8.1	12
F_3Phe	0.027 ± 0.0016	1.1 ± 0.06	0.02 - 0.09	19	8

195 Nonsense-suppression based fluorination studies were conducted for varenicline at TyrC2
196 as discussed above. The corresponding fluorination plot shows a linear trend with a 19-fold shift
197 for F_3Phe, confirming that varenicline makes a cation-π interaction with TyrC2 in α4β2 (**Table 3**,
198 **Fig 4**).

199 Varenicline was the third secondary ammonium agonist to demonstrate functional cation-
200 π interactions with both TrpB and TyrC2 in α4β2. To support the notion that a dual cation-π

interaction is associated with secondary ammonium agonists in α4β2, we transformed nicotine – which makes a single cation-π interaction at TrpB – into a secondary ammonium. Nornicotine – nicotine that has been demethylated at the pyrrolidine N – is a natural component of tobacco that is a precursor to the well-documented carcinogen *N*'-nitrosonicotine that is a byproduct of the curing process.(Siminszky et al., 2005)

Table 4. Nornicotine

TrpB	EC_{50} (μM)	n_H	I_{max} (μA)	Fold Shift	N
Trp	1.7 ± 0.1	1.3 ± 0.1	1.33 - 9.37	1	13
F_1Trp	4.6 ± 0.2	1.3 ± 0.1	0.27 - 0.9	2.8	16
F_2Trp	11 ± 0.7	1.3 ± 0.1	0.04 - 0.11	6.4	8
F_3Trp	26 ± 2	1.5 ± 0.1	0.05 - 1.28	16	16
F_4Trp	44 ± 4	1.2 ± 0.1	0.95 - 1.51	27	8

TyrC2	EC_{50} (μM)	n_H	I_{max} (μA)	Fold Shift	N
Phe	3.3 ± 0.3	1.2 ± 0.1	0.02 - 1.42	1	15
F_1Phe	5.5 ± 0.3	1.0 ± 0.1	0.04 - 0.11	1.7	11
F_2Phe	31 ± 3	1.2 ± 0.1	0.03 - 0.26	9.6	10
F_3Phe	35 ± 2	1.4 ± 0.1	0.02 - 0.14	11	12

Nornicotine is much less potent than its methylated analog, with an EC_{50} of 1.8 μM, a 20-fold greater value than for nicotine. The fluorination plot of nornicotine at TrpB shows a cation-π interaction, with F_4Trp resulting in a 27-fold shift in EC_{50}, demonstrating a functionally important cation-π interaction (**Table 4**, **Fig 3**). Results at TyrC2 show the same type of trend seen for other secondary ammonium agonists analyzed in this report, with a linear fluorination plot and a 11-fold loss of function for F_3Phe (**Table 4**, **Fig 4**).

Discussion

Structure-function studies of four different agonists with distinct overall structures but a common secondary ammonium moiety have established a functional cation-π interaction with

both TrpB and TyrC2 in α4β2 nAChRs. Nornicotine forms a cation-π interaction with TyrC2, but nicotine, which only differs from nornicotine by being a tertiary rather than secondary ammonium, does not. This nicotine/nornicotine comparison in particular presents a compelling case that the dual cation-π interaction is a consequence of the secondary ammonium group of select agonists at α4β2.

The significance of TrpB in agonist binding to nAChRs remains a central tenet of the pharmacology of this system. In a cation-π interaction, the aromatic ring of Trp is a stronger binding site that those of Tyr or Phe, regardless of the nature of the cation, but Tyr and Phe can certainly make strong cation-π interactions. (Davis and Dougherty, 2015) Early studies focused on ACh and nicotine and found that only TrpB showed a strong response to fluorination. We have now found that four other agonists show, in addition to TrpB, a significant response to fluorination at TyrC2. These four are structurally diverse, but share a common feature of being a secondary ammonium. The implication is clear that the more compact secondary ammonium is able to establish an additional interaction compared to the bulkier quaternary (ACh) or tertiary (nicotine) systems.

Two studies of the primary ammonium agonist GABA at pentameric receptors – one at the RDL insect GABA receptor and one at the prokaryotic ELIC receptor – show that this primary ammonium agonist makes functionally important cation-π interactions to the aromatics at positions B and C2 (Lummis et al., 2005; Spurny et al., 2012). Again, a more compact agonist can make a dual cation-π interaction. A recent computational study of the AChBP aromatic box suggests that the side chains of each aromatic box residue can contribute to the overall cation-π binding energy in the ACh-AChBP complex (Davis and Dougherty, 2015). However, from a

functional perspective, only TrpB is universally important, with TyrC2 being identified here as contributing in some, but not all, cases.

A popular model for nAChR gating proposes that loop C moves on agonist binding so as to clamp down on the agonist and more clearly define the aromatic box (Wang et al., 2009). This movement of loop C is proposed to be a key functional feature of the gating mechanism. It may be that with the less bulky secondary ammonium agonists, loop C is able to move closer to the agonist. This larger motion by loop C leads to a closer contact between TyrC2 and the agonist, enabling a cation-π interaction and making TyrC2 responsive to fluorination. AChBP structures with varenicline vs. nicotine bound do not show a meaningful difference in the position of loop C, but AChBP did not evolve to undergo a gating process and likely undergoes minimal conformational changes when binding small molecules (Celie et al., 2004; Rucktooa et al., 2012).

In summary, we have found a distinction in the binding mode of agonists at the α4β2 nAChR. The natural agonist ACh and the prominent component of tobacco nicotine both make a cation-π interaction to TrpB, along with other hydrogen bonding interactions. In contrast, four agonists that share a common feature of being secondary ammonium ions make a dual cation-π interaction to TrpB and TyrC2. This pattern may be unique to the α4β2 subtype, as it was not reported for TC299423 at the α6β2 subtype (Post et al., 2015). Further studies of other agonists and other subtypes could provide valuable guidance in designing more subtype-selective activators of nAChRs.

Figure Captions

Figure 1. A view of nicotine at the α4β2 binding site. The crystal structure of α4β2 (PDB 5KXI) on the left shows the aromatic box motif, with each loop contributing to the binding site in a unique color and nicotine in gray. The schematic on the right details the hydrogen bond (red) and cation-π interaction (purple) interactions previously determined for nicotine with TrpB (α4: 149), as well as how TyrC2 (α4: 197) could interact with other agonists. TyrA (α4: 93), TyrC1(α4: 190) and TrpD (β2: 57) are shown in the crystal structure but omitted from the schematic for clarity. An alignment of each loop contributing to the box in the human nAChR family is shown at the bottom.

Figure 2. The structures and electrostatic potential maps of acetylcholine and nicotine are shown here for comparison to the secondary amine agonists and have been calculated with Hartree Fock 6-31G** (shown on a scale of -10 to +150 kcal/mol)

Figure 3. Fluorination plots of all the agonists tested in this report at TrpB in α4β2. The x-axis is the predicted M06/6-31G(d,p) DFT-calculated energies between a sodium ion and each side chain (labeled) in the gas phase as described in Davis et al. The y-axis is the log of the fold-shift in EC_{50}. Each agonist tested showed a linear trend, and therefore demonstrated a functional cation-π interaction at TrpB, as previously seen with acetylcholine and nicotine. Data plotted for varenicline is from Tavares et. al.

Figure 4. Fluorination plots of all the agonists tested in this report at TyrC2 in α4β2. The x-axis is the predicted M06/6-31G(d,p) DFT-calculated energies between a sodium ion and each side chain (labeled) in the gas phase as described in Davis et al. The y-axis is the log of the fold-shift in EC_{50}. Each agonist tested shows a linear trend, and therefore demonstrates a functional cation-π interaction with TyrC2, a result not previously seen with acetylcholine or nicotine.

Figure 5. Representative traces from dose-response experiments with a variety of agonists, non-canonical amino acid substitutions, and I_{max} values

5.7 References

Blum, A.P., Lester, H.A., and Dougherty, D.A. (2010). Nicotinic pharmacophore: The pyridine N of nicotine and carbonyl of acetylcholine hydrogen bond across a subunit interface to a backbone NH. Proc. Natl. Acad. Sci. *107*, 13206–13211.

Blum, A.P., Arnam, E.B.V., German, L.A., Lester, H.A., and Dougherty, D.A. (2013). Binding Interactions with the Complementary Subunit of Nicotinic Receptors. J. Biol. Chem. *288*, 6991–6997.

Celie, P.H.N., van Rossum-Fikkert, S.E., van Dijk, W.J., Brejc, K., Smit, A.B., and Sixma, T.K. (2004). Nicotine and carbamylcholine binding to nicotinic acetylcholine receptors as studied in AChBP crystal structures. Neuron *41*, 907–914.

Coe, J.W., Brooks, P.R., Wirtz, M.C., Bashore, C.G., Bianco, K.E., Vetelino, M.G., Arnold, E.P., Lebel, L.A., Fox, C.B., Tingley, F.D., et al. (2005a). 3,5-Bicyclic aryl piperidines: a novel class of alpha4beta2 neuronal nicotinic receptor partial agonists for smoking cessation. Bioorg. Med. Chem. Lett. *15*, 4889–4897.

Coe, J.W., Brooks, P.R., Vetelino, M.G., Wirtz, M.C., Arnold, E.P., Huang, J., Sands, S.B., Davis, T.I., Lebel, L.A., Fox, C.B., et al. (2005b). Varenicline: An α4β2 Nicotinic Receptor Partial Agonist for Smoking Cessation. J. Med. Chem. *48*, 3474–3477.

Corringer, P.-J., Novère, N.L., and Changeux, J.-P. (2000). Nicotinic Receptors at the Amino Acid Level. Annu. Rev. Pharmacol. Toxicol. *40*, 431–458.

Damaj, M.I., Glassco, W., Aceto, M.D., and Martin, B.R. (1999). Antinociceptive and Pharmacological Effects of Metanicotine, a Selective Nicotinic Agonist. J. Pharmacol. Exp. Ther. *291*, 390–398.

Davis, M.R., and Dougherty, D.A. (2015). Cation–π interactions: computational analyses of the aromatic box motif and the fluorination strategy for experimental evaluation. Phys. Chem. Chem. Phys. *17*, 29262–29270.

De Biasi, M., and Dani, J.A. (2011). Reward, Addiction, Withdrawal to Nicotine. Annu. Rev. Neurosci. *34*, 105–130.

Dineley, K.T., Pandya, A.A., and Yakel, J.L. (2015). Nicotinic ACh receptors as therapeutic targets in CNS disorders. Trends Pharmacol. Sci. *36*, 96–108.

Dougherty, D.A. (1996). Cation-π Interactions in Chemistry and Biology: A New View of Benzene, Phe, Tyr, and Trp. Science *271*, 163–168.

Dougherty, D.A. (2013). The Cation−π Interaction. Acc. Chem. Res. *46*, 885–893.

318 Drenan, R.M., Grady, S.R., Whiteaker, P., McClure-Begley, T., McKinney, S., Miwa, J.M.,
319 Bupp, S., Heintz, N., McIntosh, J.M., Bencherif, M., et al. (2008). In Vivo Activation of
320 Midbrain Dopamine Neurons via Sensitized, High-Affinity α6* Nicotinic Acetylcholine
321 Receptors. Neuron *60*, 123–136.

322 Gotti, C., Zoli, M., and Clementi, F. (2006). Brain nicotinic acetylcholine receptors: native
323 subtypes and their relevance. Trends Pharmacol. Sci. *27*, 482–491.

324 Grady, S.R., Drenan, R.M., Breining, S.R., Yohannes, D., Wageman, C.R., Fedorov, N.B.,
325 McKinney, S., Whiteaker, P., Bencherif, M., Lester, H.A., et al. (2010). Structural differences
326 determine the relative selectivity of nicotinic compounds for native α4β2*-, α6β2*-, α3β4*- and
327 α7-nicotine acetylcholine receptors. Neuropharmacology *58*, 1054–1066.

328 Henderson, B.J., Srinivasan, R., Nichols, W.A., Dilworth, C.N., Gutierrez, D.F., Mackey,
329 E.D.W., McKinney, S., Drenan, R.M., Richards, C.I., and Lester, H.A. (2014). Nicotine exploits
330 a COPI-mediated process for chaperone-mediated up-regulation of its receptors. J. Gen. Physiol.
331 *143*, 51–66.

332 Holladay, M.W., Dart, M.J., and Lynch, J.K. (1997). Neuronal Nicotinic Acetylcholine
333 Receptors as Targets for Drug Discovery. J. Med. Chem. *40*, 4169–4194.

334 Jackson, K.J., Sanjakdar, S.S., Muldoon, P.P., McIntosh, J.M., and Damaj, M.I. (2013). The
335 α3β4* nicotinic acetylcholine receptor subtype mediates nicotine reward and physical nicotine
336 withdrawal signs independently of the α5 subunit in the mouse. Neuropharmacology *70*, 228–
337 235.

338 Kuryatov, A., Luo, J., Cooper, J., and Lindstrom, J. (2005). Nicotine Acts as a Pharmacological
339 Chaperone to Up-Regulate Human α4β2 Acetylcholine Receptors. Mol. Pharmacol. *68* 1839-
340 1851.

341 Le Novère, N., Corringer, P.J., and Changeux, J.P. (2002). The diversity of subunit composition
342 in nAChRs: Evolutionary origins, physiologic and pharmacologic consequences. J. Neurobiol.
343 *53*, 447–456.

344 Lummis, S.C.R., L. Beene, D., Harrison, N.J., Lester, H.A., and Dougherty, D.A. (2005). A
345 Cation-π Binding Interaction with a Tyrosine in the Binding Site of the $GABA_C$ Receptor. Chem.
346 Biol. *12*, 993–997.

347 Millar, N.S. (2003). Assembly and subunit diversity of nicotinic acetylcholine receptors.
348 Biochem. Soc. Trans. *31*, 869–874.

349 Nelson, M.E., Kuryatov, A., Choi, C.H., Zhou, Y., and Lindstrom, J. (2003). Alternate
350 Stoichiometries of α4β2 Nicotinic Acetylcholine Receptors. Mol. Pharmacol. *63*, 332–341.

351 Papke, R.L., Webster, J.C., Lippiello, P.M., Bencherif, M., and Francis, M.M. (2000). The
352 Activation and Inhibition of Human Nicotinic Acetylcholine Receptor by RJR-2403 Indicate a
353 Selectivity for the α4β2 Receptor Subtype. J. Neurochem. *75*, 204–216.

354 Post, M.R., Limapichat, W., Lester, H.A., and Dougherty, D.A. (2015). Heterologous expression
355 and nonsense suppression provide insights into agonist behavior at α6β2 nicotinic acetylcholine
356 receptors. Neuropharmacology *97*, 376–382.

357 Puskar, N.L., Lester, H.A., and Dougherty, D.A. (2012). Probing the Effects of Residues Located
358 Outside the Agonist Binding Site on Drug-Receptor Selectivity in the Nicotinic Receptor. ACS
359 Chem. Biol. *7*, 841–846.

360 Quik, M., and McIntosh, J.M. (2006). Striatal α6* Nicotinic Acetylcholine Receptors: Potential
361 Targets for Parkinson's Disease Therapy. J. Pharmacol. Exp. Ther. *316*, 481–489.

362 Quik, M., and Wonnacott, S. (2011). α6β2* and α4β2* Nicotinic Acetylcholine Receptors As
363 Drug Targets for Parkinson's Disease. Pharmacol. Rev. *63*, 938–966.

364 Romanelli, M.N., Gratteri, P., Guandalini, L., Martini, E., Bonaccini, C., and Gualtieri, F.
365 (2007). Central Nicotinic Receptors: Structure, Function, Ligands, and Therapeutic Potential.
366 ChemMedChem *2*, 746–767.

367 Rucktooa, P., Haseler, C.A., van Elk, R., Smit, A.B., Gallagher, T., and Sixma, T.K. (2012).
368 Structural Characterization of Binding Mode of Smoking Cessation Drugs to Nicotinic
369 Acetylcholine Receptors through Study of Ligand Complexes with Acetylcholine-binding
370 Protein. J. Biol. Chem. *287*, 23283–23293.

371 Siminszky, B., Gavilano, L., Bowen, S.W., and Dewey, R.E. (2005). Conversion of nicotine to
372 nornicotine in Nicotiana tabacum is mediated by CYP82E4, a cytochrome P450 monooxygenase.
373 Proc. Natl. Acad. Sci. U. S. A. *102*, 14919–14924.

374 Spurny, R., Ramerstorfer, J., Price, K., Brams, M., Ernst, M., Nury, H., Verheij, M., Legrand, P.,
375 Bertrand, D., Bertrand, S., et al. (2012). Pentameric ligand-gated ion channel ELIC is activated
376 by GABA and modulated by benzodiazepines. Proc. Natl. Acad. Sci. U. S. A. *109*, E3028–
377 E3034.

378 Tavares, X.D.S., Blum, A.P., Nakamura, D.T., Puskar, N.L., Shanata, J.A.P., Lester, H.A., and
379 Dougherty, D.A. (2012). Variations in Binding Among Several Agonists at Two Stoichiometries
380 of the Neuronal, α4β2 Nicotinic Receptor. J. Am. Chem. Soc. *134*, 11474–11480.

381 Van Arnam, E.B., and Dougherty, D.A. (2014). Functional Probes of Drug–Receptor
382 Interactions Implicated by Structural Studies: Cys-Loop Receptors Provide a Fertile Testing
383 Ground. J. Med. Chem. *57*, 6289–6300.

384 Wall, T.R. (2015). Effects of TI-299423 on Neuronal Nicotinic Acetylcholine Receptors.
385 California Institute of Technology.

386 Wang, H.-L., Toghraee, R., Papke, D., Cheng, X.-L., McCammon, J.A., Ravaioli, U., and Sine,
387 S.M. (2009). Single-Channel Current Through Nicotinic Receptor Produced by Closure of
388 Binding Site C-Loop. Biophys. J. *96*, 3582–3590.

389 Xiao, C., Srinivasan, R., Drenan, R.M., Mackey, E.D.W., McIntosh, J.M., and Lester, H.A.
390 (2011). Characterizing functional α6β2 nicotinic acetylcholine receptors in vitro: Mutant β2
391 subunits improve membrane expression, and fluorescent proteins reveal responsive cells.
392 Biochem. Pharmacol. *82*, 852–861.

393 Xiu, X., Puskar, N.L., Shanata, J.A.P., Lester, H.A., and Dougherty, D.A. (2009). Nicotine
394 binding to brain receptors requires a strong cation–π interaction. Nature *458*, 534–537.

395 Zoli, M., Pistillo, F., and Gotti, C. (2015). Diversity of native nicotinic receptor subtypes in
396 mammalian brain. Neuropharmacology *96, Part B*, 302–311.

397 Zuo, W., Xiao, C., Gao, M., Hopf, F.W., Krnjević, K., McIntosh, J.M., Fu, R., Wu, J., Bekker,
398 A., and Ye, J.-H. (2016). Nicotine regulates activity of lateral habenula neurons via presynaptic
399 and postsynaptic mechanisms. Sci. Rep. *6*, 32937.

400

401

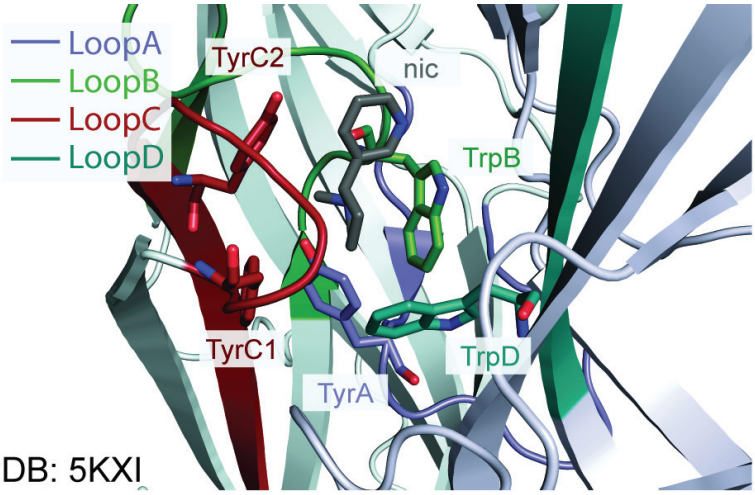

PDB: 5KXI

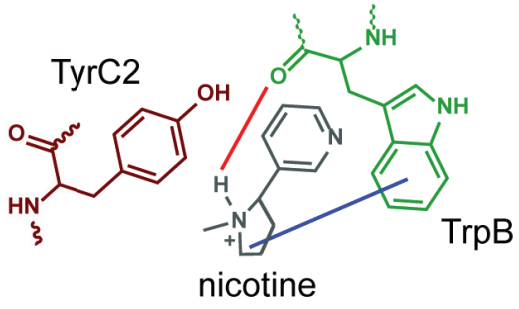

	Loop A								Loop B								Loop C								Loop D						
α1	W	R	P	D	V	V	L	Y	W	T	Y	D	G	S	V	V	Y	S	C	C	P	T	P	Y	L	D					
α2	W	I	P	D	I	V	L	Y	W	T	Y	D	K	A	K	I	Y	D	C	C	A	–	I	Y	P	D					
α3	W	K	P	D	I	V	L	Y	W	S	Y	D	K	A	K	I	Y	N	C	C	E	–	I	Y	P	D					
α4	W	R	P	D	I	V	L	Y	W	T	Y	D	K	A	K	I	Y	E	C	C	A	–	I	Y	P	D					
α6	W	K	P	D	I	V	L	Y	W	T	Y	D	K	A	E	I	Y	N	C	C	E	–	I	Y	T	D					
α7	W	K	P	D	I	L	L	Y	W	S	Y	G	G	W	S	L	Y	E	C	C	K	–	P	Y	P	D					
α9	W	R	P	D	I	V	L	Y	W	T	Y	N	G	N	Q	V	Y	G	C	C	S	–	P	Y	P	D					
α10	W	R	P	D	I	V	L	Y	W	T	H	G	G	H	Q	L	Y	G	C	C	S	–	P	Y	P	D					
γ																											W	I	E	M	Q	W
δ																											W	I	D	H	A	W
β2																											W	L	T	Q	E	W
β4																											W	L	K	Q	E	W
α7																											W	L	Q	M	S	W
α9																											W	I	R	Q	I	W
α10																											W	I	R	Q	E	W